Nanoscale Polymer Electrolytes: Ultrathin Electrodeposited Poly(Phenylene Oxide) with Solid-State Ionic Conductivity

Christopher P. Rhodes,[†] Jeffrey W. Long,*[,†] Michael S. Doescher,[†] John J. Fontanella,[‡] and Debra R. Rolison*[,†]

Naval Research Laboratory, Surface Chemistry Branch, Code 6170, Washington, DC 20375 and Physics Department, U.S. Naval Academy, Annapolis, Maryland 21402

Received: May 28, 2004

Incorporating ions within electrodeposited polymer dielectric films creates ultrathin solid electrolytes on a length scale (<50 nm) that bridges molecular electronics and conventional electrochemical devices. Electrooxidation of phenol in basic acetonitrile generates electrodeposited nanoscale (21 ± 2 nm), pinhole-free poly(phenylene oxide), PPO, films on indium−tin-oxide substrates. Solid-state electrical measurements using top electrode contacts (vapor-deposited Au, liquid Hg, or liquid Ga−In eutectic) confirm that these PPO films are electronically insulating ($7 \pm 2 \times 10^{-12}$ S cm^{-1}) with a high dielectric strength ($1.7 \pm 0.1 \times 10^6$ V cm^{-1}). The insulating film is converted to an ultrathin solid polymer electrolyte by soaking in a solution of $LiClO_4$−propylene carbonate and then heating under vacuum to remove solvent. Atomic force microscopy establishes that the salt-impregnated film is thicker (43 ± 10 nm) than the as-prepared PPO film. The X-ray photoelectron spectroscopic measurements suggest minimal retention of solvent in the film. Electrochemical impedance measurements demonstrate that the incorporated ions are mobile in the solid state with an ionic conductivity of $7 \pm 4 \times 10^{-10}$ S cm^{-1}. Such ultrathin solid polymer electrolytes should enable progress toward nanoscopic solid-state ionic devices and power sources.

Introduction

The physical and chemical manipulation necessary to create nanoelectronic devices,[1] has placed considerable focus on systems that are either electronically conducting[2−5] or insulating.[6,7] Reports are lacking of nanoscale systems that are both electronically insulating *and* ionically conducting, and therefore function as nanoscale solid electrolytes in batteries, sensors, and other solid-state ionic devices. Previous studies of solid electrolytes include nanometer-scale particles[8,9] or domains;[10] however, the overall thickness of these systems remains on the micrometer scale. Here we describe initial studies of solid electrolytes where the overall thickness of the electrolyte, and therefore the distance between the electrodes, is ≤50 nm.

Solid polymer films at this length scale are ∼20 times thinner than the 500- to 1500-nm-thick solid electrolytes used in even the best thin-film batteries,[11,12] and ∼1000 times thinner than 20- to 50-*micron*-thick electrolytes used for many systems. The development of nanostructured battery designs is specifically needed to overcome diffusion limitations that occur at high charge/discharge rates,[13,14] and to meet the power requirements of MEMS and other devices (such as "Smart Dust") that require power sources integrated on a chip,[15] but provide limited areal footprints.[16] Of practical importance, reducing the distance between the electrodes reduces the ohmic drop across the electrolyte and can increase the power and energy density of energy-storage devices.[11,12,17] Of fundamental importance is the recognition that in the regime where the distance between the electrodes is on the order of 5 to 50 nm, ionic transport can be dramatically altered because the electrical double layers overlap, thereby forming a space-charge layer and establishing field-driven fluxes within the electrolyte.[16] The study of systems with nanoscale dimensions between the electrodes represents an important contribution to the emerging field of nanoionics,[18,19] and provides experimental entry to the largely unexplored area between molecular and conventional electronics.

Electropolymerization has already been used to fabricate nanoscale polymers for numerous electronic applications including sensors,[20] catalysts,[21] and charge-storage devices;[22,23] however, its use to fabricate ultrathin solid polymer electrolytes remains unexplored. As a synthetic strategy, electropolymerization offers a number of advantages over methods such as self-assembly or vapor deposition to create nanoscale polymer films for solid electrolytes. Conformal nanoscale films with controlled thickness are generated when conditions are chosen such that a passivating polymer film is electrosynthesized via a self-limiting growth mechanism.[24] The deposited films are inherently pinhole free,[25,26] thereby eliminating electrical shorts between the electrodes. Since the film is generated directly at the electrode surface, intimate electrode−electrolyte contact occurs, which should improve charge transport in the electrode−electrolyte interfacial region.[27]

Electropolymerization is a soft chemistry route that can readily generate nanoscale, pinhole-free films on nonplanar, nonline-of-sight geometries,[28,29] unlike chemical vapor deposition and sputtering. This capability is critical in our efforts to develop solid electrolytes for nonplanar, three-dimensional (3-D) cathode−electrolyte−anode geometries where the components are interpenetrating and the distance between the electrodes remains <50 nm.[16] We previously demonstrated that electrodepositing <15-nm-thick films of proton-conductive poly(*o*-phenylenediamine) on mesoporous, 3-D nanostructured MnO_2

* Corresponding authors. E-mail: jwlong@ccs.nrl.navy.mil; rolison@nrl.navy.mil.
† Naval Research Laboratory.
‡ U.S. Naval Academy.

10.1021/jp047671u CCC: $27.50
Published on Web 08/11/2004

prevented the reductive dissolution in acid of the polymer-coated MnO_2 nanoarchitecture, indicating that the ultrathin film protected the entire 200 m^2 g^{-1} area of the mesoporous, nanoscopic MnO_2 electrode.[29]

To create highly electronically insulating ultrathin polymers, we adapted prior work on poly(phenylene oxide), PPO, as synthesized from the electrooxidation of phenol. Poly(phenylene oxide) can be made ultrathin (<10-nm thick) on Au and Pt substrates,[30] and the resulting films exhibit molecular size-selective permeabilites.[31] Electrodeposited films with a variety of functional groups, structures, and properties are available by using substituted phenol monomers.[32] The electrooxidation of a related monomer, 2,6-dimethylphenol, in basic methanol solutions yields films of poly(2,6-dimethyl-1,4-phenylene oxide), PDPO, that are ~50-nm thick and highly insulating ($\sigma_{elec} = 5 \times 10^{-16}$ S cm^{-1}) in the solid state.[33] In contrast to the numerous studies of electronically conducting electrodeposited polymers, such as polyaniline, polythiophene, and polypyrrole, there are relatively few reports on the solid-state electrical properties of highly insulating electrodeposited polymers.[34,35] Further study of these systems should also yield improved methods to produce ultrathin films for electronic insulation.[36]

In a recent study, we showed that poly(phenylene oxide) can be electrodeposited on mesoporous MnO_2 nanoarchitectures to fabricate an integrated electrode−separator nanoarchitecture with the ability to charge and discharge Li^+ in a nonaqueous electrolyte.[37] The nano-MnO_2||PPO system is a precursor to a solid-state nanostructured integrated three-dimensional battery,[16] if the PPO can be transformed into a solid-state ion conductor. Polymers may be especially useful as solid electrolytes in such designs, as the elasticity of the polymer should accommodate the volume expansion associated with cation insertion more readily than inorganic glasses or crystalline materials. Here we report the solid-state electrical properties of electrodeposited PPO on a planar oxide electrode and demonstrate the incorporation of mobile ions in the film to generate nanoscale solid polymer electrolytes.

Experimental Section

Phenol, tetrabutylammonium perchlorate, tetramethylammonium hydroxide pentahydrate, acetonitrile (HPLC grade), lithium perchlorate ($LiClO_4$), propylene carbonate (PC), sodium sulfate, mercury, and gallium−indium eutectic (Ga−In) were obtained from Aldrich. All reagents were used as received except for the salts, which were dried under vacuum at 150 °C for 12 h. The water used in all experiments was 18 MΩ cm (Barnstead NANOpure). Transparent, conducting indium−tin-oxide (ITO) films on glass substrates were obtained from Delta Technologies ($R_s = 6$ Ω). The ITO films were sonicated in a 20% ethanolamine/H_2O solution at 90 °C for 20 min, plasma cleaned for 20 min in an O_2 plasma (Harrick model PDC-3GX), and then rinsed and stored in acetonitrile. Gold slides (100-nm Au with a 5-nm Ti undercoating) were obtained from EMF, Corp. The Au slides were cleaned before use in a freshly prepared "piranha" solution (H_2SO_4:H_2O_2, 3:1 ratio)—**Warning**: highly corrosive.

The monomer solution was prepared by combining 50 mM phenol and 0.1 M tetrabutylammonium perchlorate in acetonitrile and then adding tetramethylammonium hydroxide to make the solution 50 mM in base. The ITO or Au substrates were placed in a three-electrode cell with a Pt-gauze auxiliary electrode and a silver wire reference electrode, AgQRE (−767 mV vs SSCE). The films were electrodeposited from the monomer solution using cyclic voltammetry (Radiometer potentiostat/galvanostat) at either ITO (scanning from 767 to 1767 mV at 100 mV s^{-1} for 22 cycles) or Au substrates (scanning from 567 to 1567 mV at 100 mV s^{-1} for 22 cycles). After electrodeposition, the films were rinsed in acetonitrile. For the thickness and solid-state electrical measurements of the dry PPO films, the films were evacuated overnight in a vacuum oven at room temperature. To introduce ions into the films, the PPO films were soaked in $LiClO_4$−PC for 3−4 days, rinsed by dipping the soaked film in clean propylene carbonate, and then dried under vacuum at 150 °C for 14 h.

For the permeability experiments, the as-prepared PPO films were rinsed in flowing H_2O and then placed in a three-electrode cell with a solution of 1mM bis(2,2′,2″-terpyridine) cobalt(II) perchlorate (made using minor modifications of reported procedures[38]) in an aqueous solution of 0.2 M Na_2SO_4 with Pt auxiliary and SSCE-reference electrodes. The electrode was scanned between 500 mV and −400 mV for $Co(terpy)_2^{2+}$ at a scan rate of 20 mV s^{-1}. Following this measurement, the films were rinsed with clean acetonitrile, dried under vacuum for 150 °C for 14 h, and then an identical permeability experiment was repeated.

The thickness, roughness, and surface area of the films were determined using an atomic force microscope, AFM (Digital Instruments Bioscope or Multimode), with a silicon nitride cantilever operating in tapping mode at a scan rate of 0.2−0.5 Hz. For the thickness measurements, an area of 100 μm × 100 μm was used; for roughness and surface area calculations, an area of 2 μm × 2 μm was used. The images were analyzed (Nanoscope IIIA software package) to determine thickness, roughness, and three-dimensional surface area. Roughness calculations were performed on an image that had undergone first-order flattening. For the thickness measurements, the AFM was used as a profilometer. A razor blade was used to scrape the polymer film from the ITO surface, and the film thickness for a given sample was determined as the mean of five different sections of the film using the section analysis feature of the software. To verify that minimal ITO was scraped off, the thickness of the PPO on ITO was evaluated at an edge defined by taping the substrate rather than using the razor. The razor and edge measurements were taken on the same film and gave identical thickness values within experimental error, which validates the use of the razor blade method to remove polymer to determine the thickness of the films. To obtain a mean thickness of the ITO||PPO films with ions without including the effect of salt clusters at the polymer−air interface, thickness measurements (as described above) were obtained from multiple points away from the clusters.

Deposition of Au directly on the ITO||PPO films was done using a CVC Products, Inc. filament evaporator. Gold was deposited at 0.5 Å s^{-1} at ~10^{-7} torr to a thickness of 50 nm using an Inficon XTC thin-film deposition controller. The Au pads were obtained by masking the deposition area with a wafer board containing drilled holes. The area of the deposited Au pads (2.26 ± 0.25 mm^2) was determined by measuring the diameter of the pads with an optical microscope. Contact to the Au pads was made with liquid gallium−indium eutectic on a Au wire that was positioned using a micromanipulator. To obtain a top contact with either liquid Hg or Ga−In eutectic, the liquid metal was contained in a 1-mL syringe and electrical contact to the liquid metal was made using a tungsten wire. Contacting the liquid metal to the polymer was accomplished with a micromanipulator and was evidenced by visible deformation of the liquid metal at the polymer surface.

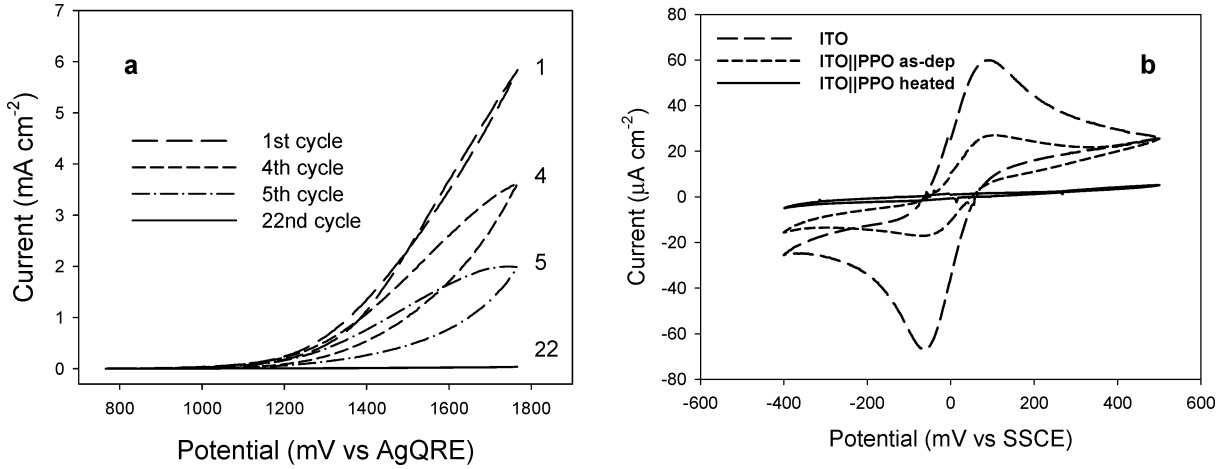

Figure 1. (a) Electrodeposition of poly(phenylene oxide) on indium−tin oxide (767−1767 mV vs AgQRE, 22 cycles at 100 mV s^{-1}); the decrease in the current with subsequent scans is characteristic of self-limiting film behavior. (b) Voltammetric response of 1 mM $Co(trpy)_2(ClO_4)_2$ in 0.2 M Na_2SO_4 at uncoated ITO, PPO-coated ITO (as-deposited), and PPO-coated ITO (heated under vacuum: 150 °C, 14 h) at 20 mV s^{-1}.

Electrical measurements were made at room temperature in an argon-filled glovebox (Vacuum Atmospheres Corp., H_2O < 10 ppm). The impedance measurements were made using 50-mV applied ac potential and 0-V applied dc bias in the frequency range 1 MHz to 100 Hz (Solartron 1260). Impedance below 100 Hz was limited by the sensitivity of the instrument above a $|Z|$ of 10^8 Ω. The impedance was fitted with equivalent circuits (chosen as described below) using Zplot (Scribner). An Andeen-Hagerling Model 2500 1-kHz automatic capacitance bridge operating in continuous measurement mode was used to measure the capacitance and loss. The dc measurements were made using an Autolab potentiostat/galvanostat model PGSTAT12.

The X-ray photoelectron spectroscopic measurements were taken on a Surface Science Instrument Model SSX-100-03 X-ray photoelectron spectrometer using an Al Kα X-ray source. The survey spectra were obtained using a single scan with a step size of 1 eV; high-resolution spectra averaged 10 or more scans, each collected with a step size of 0.1 eV. The energies of the photoelectron peaks were referenced to the C1s binding energy for adventitious carbon at 284.6 eV.

Results and Discussion

Synthesis and Characterization of Electrodeposited Poly(phenylene oxide) Films. Poly(phenylene oxide) films were electrodeposited from phenol in nonaqueous basic electrolyte at planar Au and indium−tin-oxide (ITO) electrodes using cyclic voltammetry as shown in Figure 1a for ITO.

The anodic current that results upon scanning to increasing positive potentials arises from the electrooxidation of the phenoxide to a phenoxy radical. The decreased current on subsequent scans indicates formation of a passivating film that hinders further monomer oxidation at the electrode surface. Beyond the 20th cycle, the current at 1767 mV is reduced by a factor of >100 compared to the first cycle. However, a limited degree of monomer oxidation may still occur by partition/diffusion of the monomer through the film to the electrode surface.[39] This self-limiting growth mechanism, which occurs for electronically insulating polymers deposited from a solution that allows minimal polymer swelling, generates nanometer-scale films of controlled thickness directly at the electrode surface, as demonstrated in previous studies of the electropolymerization of phenols.[30,33]

The ability to generate a pinhole-free film is crucial to the application of these systems as nanoscale electrolytes, because pinholes are potential sites for electrical shorts between electrodes spaced on the order of 5−50 nm. Previous studies examined the permeability of various redox-active probes into electrodeposited PPO on non-oxide substrates (Au and Pt), finding limited access of these probes to the metal electrode and molecular size-dependent permeabilites consistent with a pinhole-free film.[25,30,31] As-deposited PPO films on ITO (ITO||PPO) restrict access of cobalt(II)bis(2,2′,2″-terpyridine), $Co(trpy)_2^{2+}$, to the electrode surface, but not completely (Figure 1b). After heating ITO||PPO to 150 °C in a vacuum for 14 h, the $Co(trpy)_2^{2+/3+}$ redox process shuts off, demonstrating that the PPO film is pinhole free. The changes in the permeability of the film to redox-active probes induced by the heating step may result from crosslinking within the film as suggested by previous studies of substituted PPO[40] or from chain reorganization and packing effects; further work is underway, including characterization by infrared spectroscopy, to determine the effect of thermal curing on the polymer structure and properties on nanometer length scales.

Atomic force microscopy (AFM) was used to determine the thickness (Figure 2a) and morphology (Figure 3) of the as-deposited PPO films on ITO substrates. The morphology of the film is similar to the morphology of the underlying ITO substrate, as evidenced by the similar root-mean-square roughness of the two surfaces, R_{rms}(ITO) = 3.8 ± 0.8 nm and R_{rms}(ITO||PPO) = 4.2 ± 0.3 nm. The ability to conformally coat a conductive substrate with a molecularly smooth film[30,31,41] is of particular interest for uniformly coating nonplanar systems,[28,29] and not just the rough, planar systems studied here.

The PPO films electrodeposited on ITO substrates are 21 ± 2 nm thick, which is 3−4 times thicker than the 5−7-nm-thick films prepared on Au substrates using an analogous electrodeposition protocol.[30] This difference may arise from multiple factors: *(i)* the specific interactions of phenoxide at oxide vs metal surfaces,[42,43] *(ii)* organization of the oligomers as affected by surface roughness, and *(iii)* dissimilar electrode kinetics at Au and ITO for monomer oxidation.

Solid-State Impedance Measurements. The solid-state electrical properties of ultrathin PPO films on ITO and Au substrates were determined to evaluate their use as solid dielectrics and electrolytes. Obtaining a top electrical contact to nanometer-thick organics without either inducing electrical shorts in the

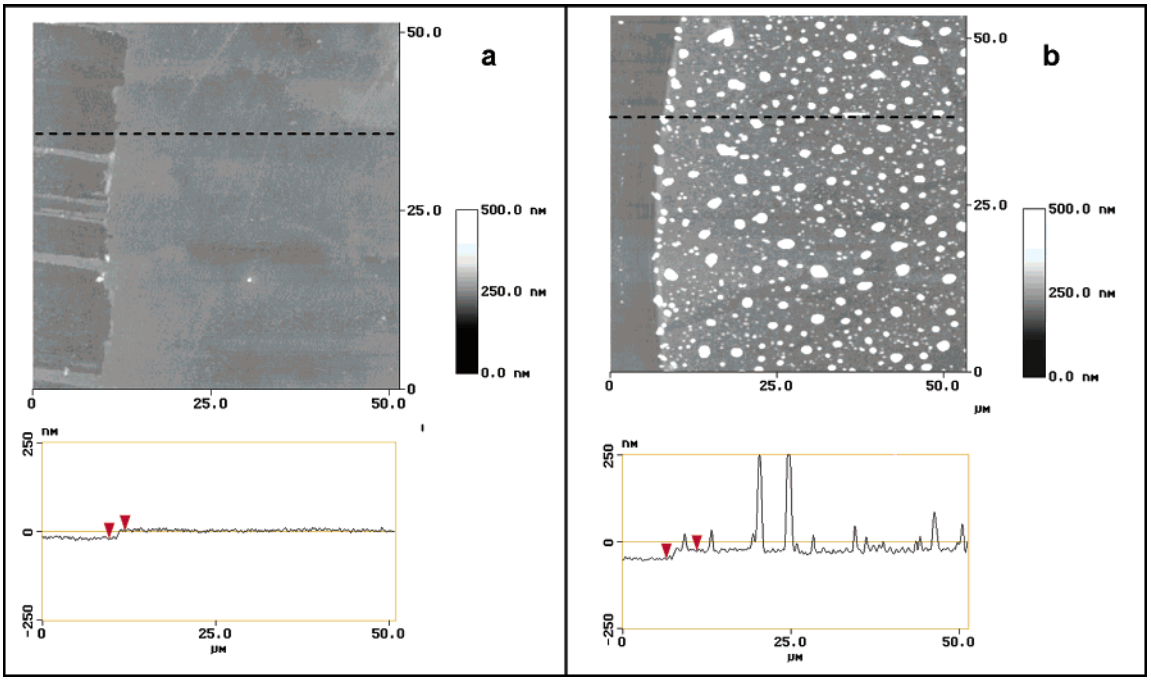

Figure 2. (a) AFM image of electrodeposited poly(phenylene oxide) film on indium−tin oxide. Areas where the razor did not completely remove the film are observed as streaks on the left side of the image. The line analysis (shown below image) taken at the position of the dotted line shows a uniform coverage of the substrate and the section analysis gave a film thickness of 21 ± 2 nm. (b) AFM image of poly(phenylene oxide) film that was soaked in lithium perchlorate-propylene carbonate (PC), rinsed in PC, and then heated at 150 °C under vacuum. The image shows the presence of clusters with diameters of ca. 0.5−2.0 μm. The line analysis (shown below image) taken at the position of the dotted line shows the height of the clusters ranges from 5−500 nm. Section analysis of film regions without the clusters resulted in a mean film thickness of 43 ± 10 nm.

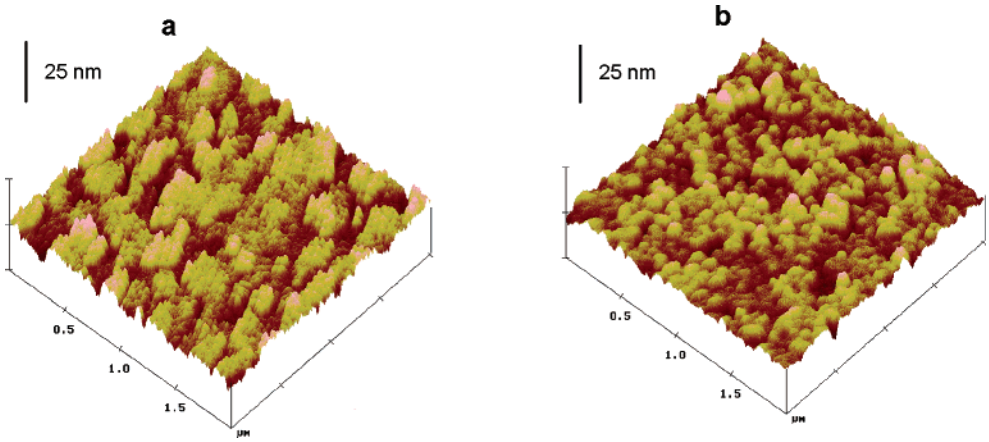

Figure 3. Atomic force microscopy images of a 2 μm × 2 μm area of (a) indium−tin-oxide (ITO) surface and (b) poly(phenylene oxide) film electrodeposited on ITO substrate.

film or changing the physicochemical nature of the organic coating is a nontrivial matter, as well documented in the recent literature on molecular electronics.[44−46] Electrical contact to self-assembled monolayers supported on conductive substrates has been made using evaporated metal,[45] conductive AFM tips,[47] and liquid metal contacts;[6,48] liquid Hg was first used to make electrical contact to fatty acid salt monolayers in the early 1970s.[49] In this study, we chose either slow evaporation of metal or micromanipulator-controlled surface approach of liquid metal to make a top electrical contact to the ultrathin polymer (schematic shown Long et al.[16]). The electronic conductivity, ionic conductivity, and dielectric strength of the electrodeposited polymer were determined by solid-state ac and dc electrical measurements (two-point probe made in an argon-filled glovebox).

The impedance of as-prepared ITO||PPO with Au, Hg, or Ga−In top contacts was obtained to determine if the top electrical contact altered the impedance response and to compare the ionic conductivity of the as-prepared film to the film after incorporating ions. The complex impedance for multiple ITO||PPO||Au samples exhibits a response consistent with that of a dielectric, as evidenced by a vertical line in the complex plane representation (Figure 4a) and a phase angle of ∼89° from 100 Hz to 10 kHz (Figure 4a, inset).

For some samples with Au top contacts, the complex impedance plot exhibited a clear deviation from a vertical line (data shown in Supporting Information), which suggests that the Au deposition process can damage the film and create charge carriers in the film or interfacial region. Similar problems with Au contacts on ultrathin organics have been reported by other groups.[45,50] The additional impedance features observed for some systems with Au top contacts complicates the determination of the properties of the polymer film itself, since the impedance results (and further characterization described below) demon-

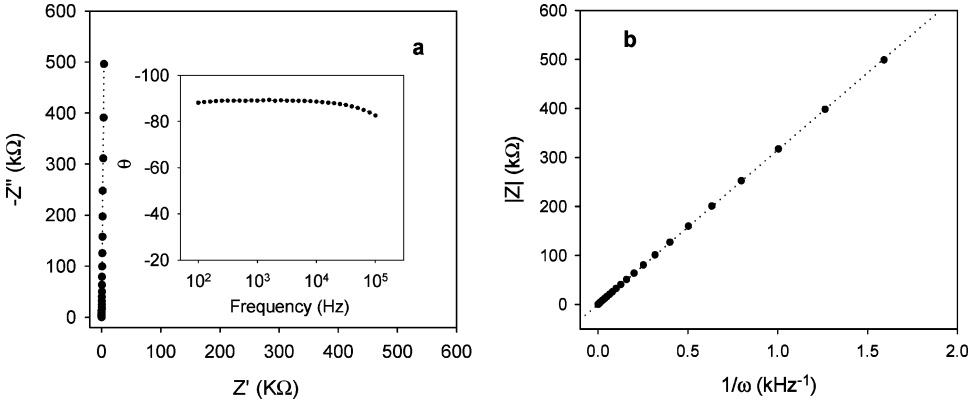

Figure 4. (a) Solid-state impedance of ITO||PPO|Au (d = 20 nm, A = 2.25 mm^2) in the frequency range 1 MHz to 100 Hz; a 50-mV-applied ac potential was used for all measurements. Inset: Bode plot representation of phase angle as a function of frequency. (b) Plot of $|Z|$ vs $1/\omega$ from solid-state impedance of ITO||PPO||Au sample (d = 20 nm, A = 2.26 mm^2); the dotted line shows the fit from linear regression.

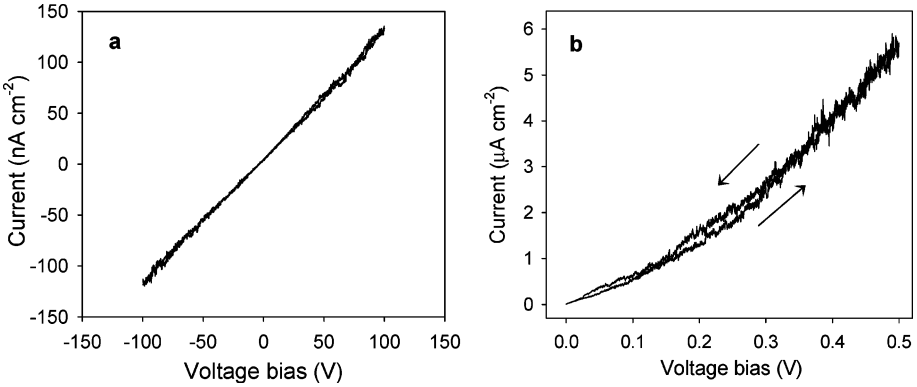

Figure 5. Solid-state dc *current*−*voltage* curves of ITO||PPO||Au (d = 21 nm, A = 2.26 mm^2); the voltage bias is with respect to Au; data were taken at 2 mV s^{-1}. (a) Voltage scan from 0 mV to 100 mV to −100 mV to 0 mV; (b) voltage scan between 0 and 500 mV; arrows indicate the direction of the scan.

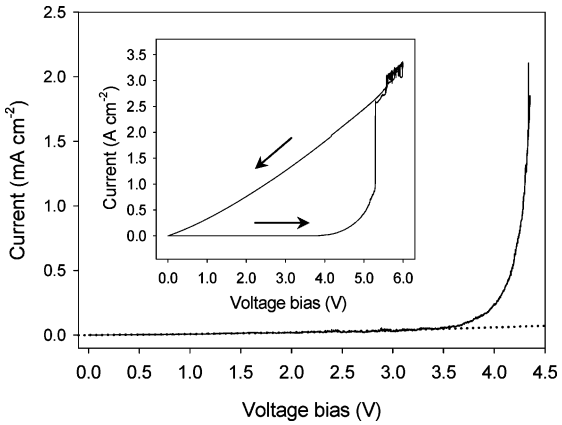

Figure 6. Solid-state dc *current*−*voltage* curves of ITO||PPO||Au (d = 20 nm, A = 2.26 mm^2) in the region 0 V to 4.2 V. The dotted line shows the fit to the I−V region from 0 to 2.5 V. The inset expands the region from 0 to 6 V, with arrows indicating direction of scan. The higher current obtained on the reverse scan (from 6 to 0 V) indicates that changes above 4 V are irreversible, which is consistent with dielectric breakdown. The data were taken at 2 mV s^{-1} with ITO positive biased.

strate that the electrical properties of the polymer film may be altered by even slow evaporative deposition of Au contacts.

To avoid the additional impedance features present for some Au contacts, the impedance of the ITO||PPO films was obtained using either Hg or Ga−In contacts. The complex impedance with a Hg (see supplemental information) or Ga−In (shown in Figure 7a) top contact exhibits a similar dielectric response to that with Au contacts demonstrating that liquid metal makes electrical contact to the film without introducing additional impedance features. Determining the contact area by direct measurements using Hg and Ga−In contacts is difficult in our experimental configuration, but initial analysis suggests that the effective contact area differs from the measured area due to poor wetting of the polymer surface by liquid Hg and Ga−In.[51]

These complications were addressed by using capacitance measurements to determine contact areas for the Hg and Ga−In top contacts. To validate this approach, the ITO||PPO||Au samples (where the contact area is known) were used to compare the experimental capacitance to the theoretical capacitance. For the ITO||PPO||Au samples that exhibited a dielectric impedance response, the film was modeled as a series RC equivalent circuit with the complex impedance described by the following equation:

$$Z^* = R_s - j\left(\frac{1}{\omega C}\right) \qquad (1)$$

where Z^* is the complex impedance, R_s is the resistance, j is $\sqrt{-1}$, ω is the value 2π times the frequency, and C is the capacitance.[52] The plot of $|Z|$ vs $1/\omega$ (Figure 4b) exhibits linear behavior and the slope of the linear regression fit was used to determine a capacitance of 129 ± 9 nF cm^{-2}. A similar equivalent circuit and procedure were used to derive the capacitance of ultrathin SAMs.[6] The accuracy of this method to determine the capacitance of our system was verified by the similarity (±3%) of the values obtained using this method to those obtained using an automatic capacitance bridge.

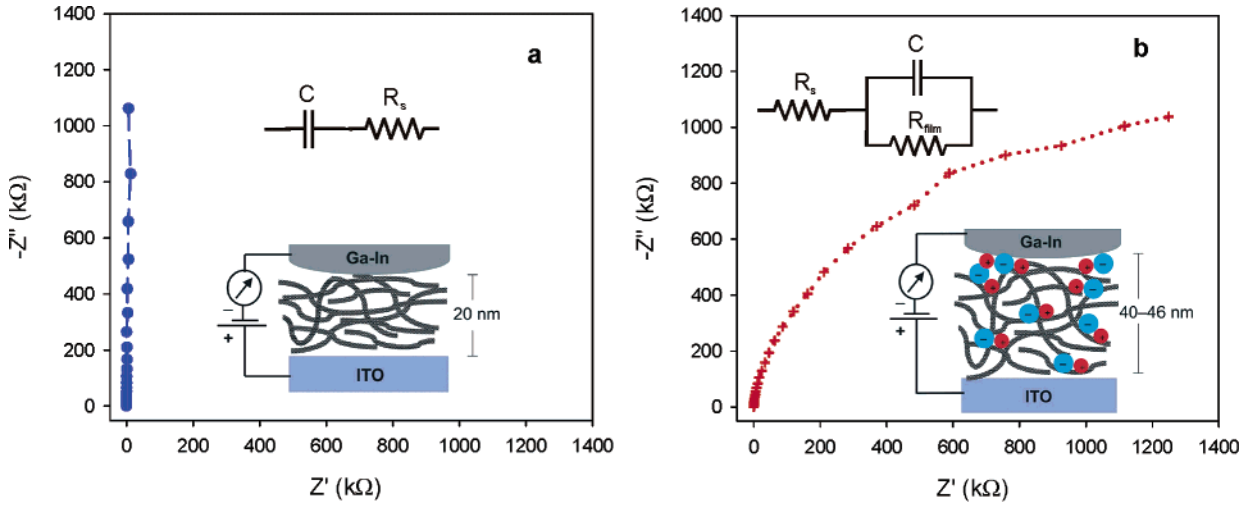

Figure 7. Solid-state impedance of (a) ITO||PPO||Ga−In and (b) ITO||PPO−$LiClO_4$||Ga−In. The data were taken in the frequency range 1 MHz to 100 Hz using a 50-mV-applied ac voltage with a 0-V-applied dc bias for all measurements. The equivalent circuits used for fitting the experimental impedance are also shown. For ITO||PPO||Ga−In, the impedance was fitted using an equivalent circuit consisting of a capacitor and resistor in series (described earlier in text). For ITO||PPO−$LiClO_4$||Ga−In, an additional resistance in parallel with the capacitance was needed to fit the impedance. Representations of the experimental configurations used for electrical measurements are shown in figure insets. The representation of ITO||PPO−$LiClO_4$||Ga−In includes ions within and on the surface of the poly(phenylene oxide) film, consistent with the XPS and AFM data.

The experimental capacitance was compared to the theoretical capacitance C_{theor} predicted for a dielectric between two electrodes, which can be described by

$$C_{\text{theor}} = \frac{\epsilon\epsilon_0 A}{d} \qquad (2)$$

where ϵ is the effective dielectric constant of the medium, ϵ_0 is the permittivity of free space, A is the area, and d is the distance between the electrodes.[52] The theoretical capacitance as calculated from eq 2 was within 7% of the experimental capacitance using the mean of the reported dielectric constants of PDPO (2.58−2.96),[53,54] the thickness determined from AFM measurements, and the area of the Au pad (corrected for the effect of surface roughness on the three-dimensional area[55]). On the basis of this agreement, which is within experimental error, the experimental capacitance and eq 2 were used to derive the contact area for the Hg and Ga−In contacts to then calculate electronic and ionic conductivity. A further complication in estimating the effective contact area of the rough ITO substrate may arise because of the presence of insulating organics at the ITO surface, which can alter the electroactive surface area.[56]

Solid-State Electrical Conductivity Measurements. Both dc and ac methods were used to determine the electronic conductivity (σ_{elec}) of the vacuum-dried, as-deposited films. Low electronic conductivity is particularly important to prevent self-discharge in energy-storage systems, and the relative importance of a highly insulating film is magnified when the electrodes are within 50 nm of each other. For solid-state dc *current−voltage* (I−V) measurements of ITO||PPO||Au and ITO||PPO||Hg samples, the current at a small applied voltage (<0.1 V) is reversible and ohmic (Figure 5a), which is consistent with electronic conduction. Ohmic behavior at low applied voltage was previously observed for electrodeposited PDPO films (180-nm thick)[34] and insulating SAMs.[7] Using Ohms' law, σ_{elec}(dc) values of $6 \pm 4 \times 10^{-12}$ and $7 \pm 3 \times 10^{-12}$ S cm^{-1} are obtained using Au or Hg top contacts, respectively (Table 1). At applied dc voltages of 0.1 to 0.5V, the I−V curves measured for our ~20-nm-thick electrodeposited PPO films with Au top contacts show a reversible and nonohmic leakage current (Figure 5b).

TABLE 1: Solid-State Electrical Conductivity of ITO||PPO||M (M=Au, Hg, Ga−In) Evaluated Using dc and ac Methods

top electrical contact	σ_{elec}(dc)/ S cm^{-1}	σ_{elec}(ac)/ S cm^{-1}
Au	$6 \pm 4 \times 10^{-12}$	$4 \pm 2 \times 10^{-11}$
Hg	$7 \pm 3 \times 10^{-12}$	$5 \pm 3 \times 10^{-12}$
Ga−In	-	$7 \pm 2 \times 10^{-12}$

Studies of related systems suggest that electronic conduction occurs via Poole−Frenkel or Schottky conduction mechanisms,[34,35] which arise from ionization of impurities in an electric field or electron transfer over the barrier height, respectively, and can exhibit linear I−V behavior at low applied fields and nonlinear I−V behavior at higher applied fields.[57] The similar values of σ_{elec}(dc) obtained with Au or Hg contacts, which have different work functions (E_F(Au, polycrystalline) = 5.1 eV, E_F(Hg) = 4.49 eV),[58] suggests that the dominant conduction mechanism at these field strengths (5×10^4 V cm^{-1}) and temperature (300 K) may be Poole−Frenkel-type conduction. However, the potential barrier height for charge injection can deviate significantly from that predicted using the Fermi levels of isolated materials evaluated in a vacuum as nonideal interfacial contact, localized interfacial charge carrier states, and image potentials may occur.[59] For our systems, a nonideal interface, and thus barrier height for the polymer−Au interface, is supported by the impedance and capacitance bridge measurements (described below), and therefore further study of the system is needed to determine the conduction mechanisms as a function of the Fermi level of the metal contact, electric field strength, and temperature.

Because dc methods may convolve contact resistance into the measured results, we also used a capacitance bridge to measure the electronic conductivity of the polymer films (see Table 1). The capacitance bridge measurement results in a more accurate determination of the film resistance because the instrument's bridge-balancing algorithm measures the film resistance (and capacitance) without including stray resistances.[60,61] With Hg contacts, ac and dc methods yield similar conductivity values, confirming that contact resistance did not significantly affect the dc measurements. However for the Au contacts, σ_{elec}(ac) is approximately an order of magnitude

higher than σ_{elec}(dc). This discrepancy indicates that the nature of the interface is altered during deposition of the Au contacts even though the variable frequency impedance from 100 Hz to 1 MHz remains consistent with that of a dielectric. Similar values of $\sigma_{elec} = 5 \pm 3 \times 10^{-12}$ and $7 \pm 2 \times 10^{-12}$ S cm^{-1} are obtained with either Hg or Ga−In top contacts, respectively; therefore, electrodeposited PPO functions as an effective electronic insulator in the solid state. Similar electronic conductivities were reported for 120-nm-thick films electrodeposited from aromatic amine monomers (5×10^{-13} S cm^{-1}),[62] with lower σ_{elec} values reported for 50-nm-thick electrodeposited PDPO (5×10^{-16} S cm^{-1}).[33]

The higher electronic conductivity of our ultrathin electrodeposited PPO films compared to prior PDPO films may result from a number of factors. One possibility is that the two-point probe configuration may overestimate the conductivity of the films due to the inclusion of surface effects in the measured resistance. Alternatively, the inherent conductivity of PPO films may be higher than PDPO films due to different coupling reactions between phenols and 2,6-substituted phenols,[53] the incorporation of side products with higher conductivities,[33] or impurities within the film.[63]

Dielectric Breakdown. For application of these films as solid electrolytes in batteries, the polymer film must have a dielectric strength compatible with the operating voltage of the device, which is ∼ 3−4 V in current Li battery designs. The dielectric strength also provides a lower limit on the film thickness needed to sustain a given electrical field between the electrodes and permits the film thickness to be included in a rational design of nanoscale dielectrics and electrolytes. For 3 V applied across a 20-nm-thick film, the electric field between the electrodes is 1.5×10^6 V cm^{-1}, which approaches or exceeds the dielectric strength of many materials.[64] The dielectric breakdown field for ultrathin PPO, taken as the point of deviation from a second-order polynomial fit of the current trace (see dotted line in Figure 6), is $1.7 \pm 0.1 \times 10^6$ V cm^{-1}. The additional current above the breakdown field results in irreversible changes in the current response of the film (Figure 6 inset), which is consistent with dielectric breakdown. The measured dielectric strength of 20-nm-thick PPO is similar to previously reported dielectric strengths of 2.3×10^6 V cm^{-1} for 3-μm-thick electrodeposited PDPO[65] and 1.5×10^6 V cm^{-1} for 120-nm-thick films electrodeposited from arylamines.[62] These results demonstrate that the dielectric properties of these systems are retained in nanometer-scale films and are comparable to films 10−100 times thicker. Given the measured dielectric strength of ultrathin PPO, a film thickness ≥18 nm is required to sustain 3 V across the film without dielectric breakdown.

Obtaining Ions in the Dry Polymer Film. For the electrodeposited polymer film to function as a solid electrolyte rather than a solid dielectric, the polymer film must conduct ions as well as serve as an electronic insulator between the active electrodes. The as-deposited dry PPO films do not contain ions (other than trace), as evidenced by the impedance response. We have considered a number of different strategies to obtain mobile ions within the film, including using substituted phenol monomers with ionic functionality,[32,66] chemically derivatizing the polymer after electrodeposition, and introducing dissolved ions in the film. Dissolving ions within polymers, extensively researched in poly(ethylene oxide), PEO, systems,[67] is perhaps the simplest route. It also has the advantage of preserving the electrical insulation of the film, whereas other methods may result in films with higher electronic conductivities.

Previous reports demonstrated that electrodeposited PPO and PDPO films are permeable to solvated ions,[31,37,68] which suggests that ions such as Li^+ (and the corresponding anion) may be incorporated simply by soaking the film in an ion-containing solution. The propensity of the polymer to accommodate ions is also influenced by the interaction of the solvent with the polymer chains. The permeability of electrodeposited PPO films to solvated ions is at least 200 times greater in acetonitrile than in H_2O, which is attributed to solvation of the polymer by acetonitrile.[31] To immobilize ions within a polymer, an ideal solvent should induce limited swelling of the polymer (without dissolution) and have a low boiling point to facilitate removal of the solvent under vacuum. On the basis of our permeability studies, which show that a heating step reduces the permeability of the PPO film to solvated ions (Figure 2b), we first soaked the film in electrolyte prior to the heating step to maximize the incorporation of ions within the polymer.

The as-deposited electrodeposited PPO films were immersed in a solution of $LiClO_4$−propylene carbonate (PC) for 3−4 days, rinsed with neat PC, and then heated (100−130 °C) under vacuum for 14 h to remove the solvent. The X-ray photoelectron spectra of ITO||PPO−$LiClO_4$ films (see Supporting Information) exhibit photoelectron peaks in the C1s and O1s regions at binding energies consistent with the structure of PPO[30] and peaks in the Li1s and Cl2p regions with binding energies consistent with those obtained for $LiClO_4$. The absence of a C1s peak at ∼292.5 eV, corresponding to the binding energy of the carbonyl carbon of propylene carbonate,[69] indicates that PC is not present in the information depth probed by XPS (estimated to be ∼8 nm)[70,71] and suggests that the polymer−salt system is not plasticized by residual solvent in the XPS sampling region.

An AFM examination of ITO||PPO−$LiClO_4$ films (Figure 2b) shows the presence of solid clusters on the polymer surface, presumably of the $LiClO_4$ salt. The size of the clusters is ∼0.5−2 μm in diameter with heights of ∼ 5−500 nm. The mean film thickness in cluster-free regions is 43 ± 10 nm, which is roughly twice that of the as-deposited ITO||PPO films (21 ± 2 nm). The increase in film thickness for ITO||PPO−$LiClO_4$ compared to ITO||PPO suggests that salt and/or solvent are present within the polymer film. The ether oxygens of poly(phenylene oxide) may solvate Li^+ in a manner similar to PEO[72,73] and other ether-containing polymers; however, further characterization is needed to determine the nature of the polymer−salt interaction.

Solid-State Impedance of Ion-Containing Poly(phenylene oxide). After soaking PPO films in $LiClO_4$−PC solutions, the impedance response of the vacuum-dried films converts from a solid dielectric to an ion conductor (compare the impedance of the as-deposited PPO film with and without ions in Figure 7), indicating that mobile ions are incorporated into the film. However, an inhomogeneous distribution of charge carriers was found by sampling different areas of the same film, with some regions exhibiting impedances that are similar to a PPO film that was not soaked in $LiClO_4$−PC. For the ITO||PPO−$LiClO_4$||GaIn samples where the impedance clearly deviates from pure dielectric behavior, the data are fitted to the equivalent circuit for an ionic conductor[52] (Figure 7b, inset), which includes an additional resistance in parallel with the capacitance. The ionic conductivity of the films was determined using the calculated resistance from the impedance, the calculated contact area,[74] and the sample thickness measured by AFM. For four independent samples, the ionic conductivity is 7 ± 4

$\times 10^{-10}$ S cm^{-1}, which is within the lower range of ionic conductivities of PEO−salt complexes at room temperature.[75]

Indium−tin-oxide electrodes are nonblocking with respect to ions and can undergo surface reactions with Li-containing electrolytes,[76] potentially complicating the impedance analysis by introducing an additional parallel RC element into the equivalent circuit. To discount these effects, analogous experiments were performed on blocking Au substrates with ∼12-nm-thick PPO films. Initial experiments of the solid-state frequency-dependent impedance of Au||PPO−$LiClO_4$||GaIn samples showed a similar response to ITO||PPO−$LiClO_4$||GaIn (shown in Figure 7b), which suggests that the mobile ions are associated with the polymer rather than the ITO substrate.

Conclusions

Electrodeposited poly(phenylene oxide) films generated on ITO substrates are ultrathin (21 ± 2 nm) and pinhole free. The solid-state electrical measurements demonstrate that the films are highly electronically insulating at $7 \pm 2 \times 10^{-12}$ S cm^{-1}, with a dielectric strength of 1.7 ± 0.1 MV cm^{-1}, permitting potential application of such ultrathin polymers as nanoscale solid dielectrics and electrically insulating coatings. Electrodeposited PPO films can be doped with ions by soaking the film in an electrolyte, such as $LiClO_4$−propylene carbonate, followed by vacuum removal of the solvent. The AFM measurements show that ion-containing films are thicker (at 43 ± 10 nm) compared to as-prepared films (21 ± 2 nm), which suggests that ions are present within the film and not just adsorbed at the polymer surface. Solid-state impedance confirms that the film with ions is a solid electrolyte with an ionic conductivity of $7 \pm 4 \times 10^{-10}$ S cm^{-1}. This study demonstrates that pinhole-free nanometer-thick solid polymer electrolytes are achievable.

The solubility limit of poly(phenylene oxide) to dissolve ions in the dry state may be much lower than poly(ethylene oxide) and other polymer systems. Using substituted phenol monomers that contain side groups with both fixed anions and ion-solvating moieties may permit the electrodeposition of nanoscale solid polymer electrolytes with high ionic conductivities. Note that because these solid electrolytes are 10−100 times thinner than standard solid electrolytes, a low ionic conductivity that would be resistively prohibitive in a 1-μm-thick film can be tolerated in a 20-nm-thick film. In our current experiment, the type of rinsing may also influence the distribution of salt in the final system since there is competitive solvation of ions by the solvent and the polymer. Further work is underway to determine the nature of the polymer−salt interaction, to characterize the inhomogeneous distribution of charge carriers in the film, and to determine the effect of ions on the dielectric breakdown.

The ability to generate nanometer-thick solid polymer electrolytes extends the emerging field of nanoionics by providing the opportunity to study ionic transport where the distance between the electrodes is on the order of 50 nm. Electropolymerization offers a fabrication method to assemble solid-state ionic devices with nanoscale dielectrics and solid electrolytes in both planar and nonplanar (3-D) geometries. We are currently working on electrodeposited polymer films that are more highly electronically insulating, exhibit higher ionic conductivities, and demonstrate solid-state charge−discharge cycling in planar configurations.

Acknowledgment. This work was supported by the U.S. Office of Naval Research and the Office of the Secretary of Defense ONR-MURI Program on 3-D Architectures for Future Electrochemical Power Sources. C.P.R. is an ONR-MURI postdoctoral associate and thanks Professor Bruce Dunn (UCLA) for useful discussions and UCLA for financial support.

Supporting Information Available: X-ray photoelectron spectroscopic measurements and additional impedance data. This material is available free of charge via the Internet at http://pubs.acs.org.

References and Notes

(1) Joachim, C.; Gimzewski, J. K.; Aviram, A. *Nature* **2000**, *408*, 541.
(2) Simon, U. *Adv. Mater.* **1998**, *10*, 1487.
(3) Schmid, G.; Liu, Y.-P.; Schumann, M.; Raschke, T.; Radehaus, C. *Nano Lett.* **2001**, *1*, 405.
(4) Cui, Y.; Lieber, C. M. *Science* **2001**, *291*, 851.
(5) Zamborini, F. P.; Leopold, M. C.; Hicks, J. F.; Kulesza, P. J.; Malik, M. A.; Murray, R. W. *J. Am. Chem. Soc.* **2002**, *124*, 8958.
(6) Rampi, M. A.; Schueller, O. J. A.; Whitesides, G. M. *Appl. Phys. Lett.* **1998**, *72*, 1781.
(7) Holmlin, R. E.; Haag, R.; Chabinyc, M. L.; Ismagilov, R. F.; Cohen, A. E.; Terfort, A.; Rampi, M. A.; Whitesides, G. M. *J. Am. Chem. Soc.* **2001**, *123*, 5075.
(8) Croce, F.; Appetecchi, G. B.; Persi, L.; Scrosati, B. *Nature* **1998**, *394*, 456.
(9) Sata, N.; Eberman, K.; Eberl, K.; Maier, J. *Nature* **2000**, *408*, 946.
(10) Soo, P. P.; Huang, B. Y.; Jang, Y. I.; Chiang, Y.-M.; Sadoway, D. R.; Mayes, A. M. *J. Electrochem. Soc.* **1999**, *146*, 32.
(11) Birke, P.; Salam, F.; Doring, S.; Weppner, W. *Solid State Ionics* **1999**, *118*, 149.
(12) Bates, J. B.; Dudney, N. J.; Neudecker, B.; Ueda, A.; Evans, C. D. *Solid State Ionics* **2000**, *135*, 33.
(13) Sides, C. R.; Li, N.; Patrissi, C. J.; Scrosati, B.; Martin, C. R. *MRS Bull.* **2002**, *27*, 604.
(14) Arora, P.; Doyle, M.; Gozdz, A. S.; White, R. E.; Newman, J. *J. Power Sources* **2000**, *88*, 219.
(15) Koeneman, P. B.; Busch-Vishniac, I. J.; Wood, K. L. *J. Microelectromech. Syst.* **1997**, *6*, 355.
(16) Long, J. W.; Dunn, B.; Rolison, D. R.; White, H. S. *Chem. Rev.*, in press.
(17) Thomas, K. E.; Sloop, S. E.; Kerr, J. B.; Newman, J. *J. Power Sources* **2000**, *89*, 132.
(18) Maier, J. *Solid State Ionics* **2002**, *154*, 291.
(19) Maier, J. *Solid State Ionics* **2003**, *157*, 327.
(20) Janata, J.; Josowicz, M. *Nature Mater.* **2003**, *2*, 19.
(21) Bettelheim, A.; White, B. A.; Raybuck, S. A.; Murray, R. W. *Inorg. Chem.* **1987**, *26*, 1009.
(22) Novak, P.; Muller, K.; Santhanam, K. S. V.; Haas, O. *Chem. Rev.* **1997**, *97*, 207.
(23) Talbi, H.; Just, P. E.; Dao, L. H. *J. Appl. Electrochem.* **2003**, *33*, 465.
(24) Murray, R. W. *Annu. Rev. Mater. Sci.* **1984**, *14*, 145.
(25) Pressprich, K. A.; Maybury, S. G.; Thomas, R. E.; Linton, R. W.; Irene, E. A.; Murray, R. W. *J. Phys. Chem.* **1989**, *93*, 5568.
(26) Finklea, H. O.; Snider, D. A.; Fedyk, J. *Langmuir* **1990**, *6*, 371.
(27) Kerr, J. B.; Sloop, S. E.; Liu, G.; Han, Y. B.; Hou, J.; Wang, S. *J. Power Sources* **2002**, *110*, 389.
(28) Liu, C.; Espenscheid, M. W.; Chen, W. J.; Martin, C. R. *J. Am. Chem. Soc.* **1990**, *112*, 2458.
(29) Long, J. W.; Rhodes, C. P.; Young, A. L.; Rolison, D. R. *Nano Lett.* **2003**, *3*, 1155.
(30) McCarley, R. L.; Thomas, R. E.; Irene, E. A.; Murray, R. W. *J. Electroanal. Chem.* **1990**, *290*, 79.
(31) McCarley, R. L.; Irene, E. A.; Murray, R. W. *J. Phys. Chem.* **1991**, *95*, 2492.
(32) Pham, M. C.; Lacaze, P. C.; Dubois, J. E. *J. Electroanal. Chem.* **1978**, *86*, 147.
(33) Oyama, N.; Ohsaka, T.; Ohnuki, Y.; Suzuki, T. *J. Electrochem. Soc.* **1987**, *134*, 3068.
(34) Dubois, J. E.; Tourillon, G.; Pham, M. C.; Lacaze, P. C. *Thin Solid Films* **1980**, *69*, 141.
(35) Tourillon, G.; Dubois, J. E.; Lacaze, P. C. *Thin Solid Films* **1980**, *65*, 91.
(36) Lewis, T. J. *IEEE Trans. Dielectr. Electron. Insul.* **1994**, *1*, 812.
(37) Rhodes, C. P.; Long, J. W.; Doescher, M. S.; Dening, B. M.; Rolison, D. R. *J. Non-Cryst. Solids*, in press.
(38) Musumeci, S.; Rizzarelli, E.; Sammartano, S.; Bonomo, R. P. *J. Electroanal. Chem.* **1973**, *46*, 109.
(39) Brumfield, J. C.; Goss, C. A.; Irene, E. A.; Murray, R. W. *Langmuir* **1992**, *8*, 2810.
(40) Mengoli, G.; Bianco, P.; Daolio, S.; Munari, M. T. *J. Electrochem. Soc.* **1981**, *128*, 2276.

(41) Goss, C. A.; Brumfield, J. C.; Irene, E. A.; Murray, R. W. *Langmuir* **1992**, *8*, 1459.
(42) Gattrell, M.; Kirk, D. W. *J. Electrochem. Soc.* **1993**, *140*, 1534.
(43) Richard, K. M.; Gewirth, A. A. *J. Phys. Chem.* **1995**, *99*, 12288.
(44) Collier, C. P.; Wong, E. W.; Belohradsky, M.; Raymo, F. M.; Stoddart, J. F.; Kuekes, P. J.; Williams, R. S.; Heath, J. R. *Science* **1999**, *285*, 391.
(45) Metzger, R. M.; Xu, T.; Peterson, I. R. *J. Phys. Chem. B* **2001**, *105*, 7280.
(46) de Boer, B.; Frank, M. M.; Chabal, Y. J.; Jiang, W. R.; Garfunkel, E.; Bao, Z. *Langmuir* **2004**, *20*, 1539.
(47) Wold, D. J.; Frisbie, C. D. *J. Am. Chem. Soc.* **2001**, *123*, 5549.
(48) Slowinski, K.; Fong, H. K. Y.; Majda, M. *J. Am. Chem. Soc.* **1999**, *121*, 7257.
(49) Mann, B.; Kuhn, H. *J. Appl. Phys.* **1971**, *42*, 4398.
(50) Zhou, C.; Deshpande, M. R.; Reed, M. A.; Jones, L., II; Tour, J. M. *Appl. Phys. Lett.* **1997**, *71*, 611.
(51) Shimizu, R. N.; Demaquette, N. R. *J. Appl. Polym. Sci.* **2000**, *76*, 1831.
(52) *Impedance Spectroscopy*; MacDonald, J. R., Ed.; John Wiley & Sons: New York, 1987; p 346.
(53) Bruno, F.; Pham, M. C.; Dubois, J. E. *Electrochim. Acta* **1977**, *22*, 451.
(54) Babai, M.; Gottesfeld, S. *Surf. Sci.* **1980**, *96*, 461.
(55) The effective contact area is slightly larger than the measured area of the Au pads due to surface roughness. For ITO, the three-dimensional area (as measured by AFM) was 7.7% higher than the two-dimensional area, and for PPO the three-dimensional area was 5.9% higher than the two-dimensional area. To account for this factor, the area of the Au pad was multiplied by a factor of 1.08.
(56) Armstrong, N. R.; Carter, C.; Donley, C.; Simmonds, A.; Lee, P.; Brumbach, M.; Kippelen, B.; Domercq, B.; Yoo, S. Y. *Thin Solid Films* **2003**, *445*, 342.
(57) Bunget, I.; Popescu, M. *Physics of Solid Dielectrics*; Elsevier: New York, 1984.
(58) *CRC Handbook of Chemistry and Physics*; Weast, R. C., Ed.; CRC Press: Boca Raton, 1987.
(59) Scott, J. C. *J. Vac. Sci. Technol., A* **2003**, *21*, 521.
(60) Foote, M. C.; Anderson, A. C. *Rev. Sci. Instrum.* **1987**, *58*, 130.
(61) Adams, E. D. *Rev. Sci. Instrum.* **1993**, *64*, 601.
(62) Volkov, A.; Tourillon, G.; Lacaze, P. C.; Dubois, J. E. *J. Electroanal. Chem.* **1980**, *115*, 279.
(63) Lacaze, P. C.; Dubois, J. E.; Tourillon, G. *Thin Solid Films* **1980**, *66*, 159.
(64) Whitehead, S. *Dielectric Breakdown of Solids*; Oxford University Press: Oxford, UK, 1951.
(65) Adohi, B.; Gosse, J. P.; Gosse, B. *J. Phys. III* **1991**, *1*, 1623.
(66) Potje-Kamloth, K.; Josowicz, M. *Ber. Bunsen-Ges. Phys. Chem.* **1992**, *96*, 1004.
(67) Gray, F. M. *Solid Polymer Electrolytes: Fundamentals and Technological Applications*; VCH: New York, 1991.
(68) Ohsaka, T.; Hirokawa, T.; Miyamoto, H.; Oyama, N. *Anal. Chem.* **1987**, *59*, 1758.
(69) Wang, K. L.; Ross, P. N. *Surf. Sci.* **1996**, *365*, 753.
(70) Tanuma, S.; Powell, C. J.; Penn, D. R. *Surf. Interface Anal.* **1994**, *21*, 165.
(71) Powell, C. J.; Jablonski, A.; Tilinin, I. S.; Tanuma, S.; Penn, D. R. *J. Electron Spectrosc.* **1999**, *99*, 1.
(72) Schantz, S.; Sandahl, J.; Borjesson, L.; Torell, L. M.; Stevens, J. R. *Solid State Ionics* **1988**, *28*−*30*, 1047.
(73) Bruce, P. G.; Vincent, C. A. *J. Chem. Soc., Faraday Trans.* **1993**, *89*, 3187.
(74) The use of $\epsilon = 2.77$ for the PPO−$LiClO_4$ system to estimate the Ga−In eutectic contact area is an approximation since the presence of ions in the film will slightly alter the dielectric constant compared to PPO film without ions.
(75) Munshi, M. Z. A.; Owens, B. B. *Polymer J.* **1988**, *20*, 577.
(76) Bressers, P. M. M. C.; Meulenkamp, E. A. *J. Electrochem. Soc.* **1998**, *145*, 2225.